Transmitter Based Look-Up Tables for Optical Wireless IR-UWB Systems

Mohammed Al-Olofi, Andreas Waadt, Guido H. Bruck, and Peter Jung
Department of Communication Technologies
University of Duisburg-Essen
Duisburg, Germany
Email: info@kommunikationstechnik.org

***Abstract*—This paper investigates a design for impulse radio ultra-wideband communication over optical wireless link using optical front-ends. The migration between IR-UWB and optical wireless communications introduces a solution for radio spectrum congestion and limited IR-UWB transmission power governed by spectrum mask. Nevertheless, the nonlinear effects of light emitting diodes (LED) limit the power dynamic range that modulates signal pulses. In this work, a transmitter based digital look-up table (LUT) is proposed. This transmitter allows of storing pulse samples values in form of binary codewords. The LUT's binary output switches LEDs groups and hence controls transmission power. This parallel switching enables power-efficient optical representation of pulses and avoids the nonlinear effects caused by LED operation characteristics. The utilization of LUT excludes the necessity of digital to analog converter (DAC) or transconductance amplifier (TCA) employed in common optical transmitters to perform the electrical-optical conversion. The selection of codeword length and LUT size are done based the BER performance generated by computer simulations. Moreover, the channel effects in presence of line of sight (LOS) and diffuse links are simulated and analyzed. The system simulations are described for a mobile user in indoor office environment. The BER performances for different mobility scenarios will be discussed.**

Keywords-Hybrid Optical/Radio systems, IR-UWB, LUT, OWC.

I. INTRODUCTION

The optical wireless communications (OWC) is an alternative technology to radio communications, which suffers from congested frequency bands as the number of mobile users increased significantly. The OWC offers a broad unlicensed free spectrum that enables high data rate, low cost, high speed, and ease of development systems. These advantages make the optical solution attractive for short range communications applications, such as smart homes, smart offices, wireless LANs, and sensor networks.

Currently, the ultra-wideband systems are the best technology choice for short range communication, since they offer a large bandwidth (3.1-10.6 GHz), high speed, immune to multipath fading, multi access capabilities, and low cost transceivers. The fractional bandwidth of UWB is defined by FCC as a signal with 20% of its center frequency or 500 MHz bandwidth, when the center frequency is above 6 GHz with a limited power levels regulated by authorities. The frequency and power regulations are different from region to region, which make the standardization of such technology a difficult task. Also, the different emission power levels increase the interference levels from UWB devices on other wireless devices operates in the same frequency band.

On other hand and a solution to these limitations, the optical link is a promising media for short range wireless communications since its offer an unlicensed free spectrum. The evaluations of using an optical media in IR-UWB systems will overcame the limitations in emission power and bandwidth and/or introduce a new radio/optical IR-UWB system that exploit the advantages of both configurations. In [1], we had proposed a design for optical IR-UWB system design to solve the problem of radio interference and enlarge the transmission power and frequency spectrum. However, the current optical sources introduce a low modulation bandwidth, which does not exceed 20 MHz in case of using LEDs and hence limit the data rate and available broadband spectrum. This limitation is caused by the characteristics of LEDs available in the market, which have a slow response to the feeding current. The 3dB frequency and hence the modulation bandwidth depends on minority carrier lifetime, which define the rise and fall time of LED. Nevertheless, a higher frequency modulation bandwidth LEDs in the range of 200–300 MHz was proposed in [2]. In this literature, a GaN-based blue LED with a higher optical output power of 1.6 mW at bias current of 35 mA and a high electrical-to-optical 3dB bandwidth of 225.4 MHz was reported. These LEDs have a smaller chip size and exhibited a lower optical output power. Commonly, a lot of solid state electronics researches focus on LED designed for OWC applications, which gives a sign that we will see high-speed low-cost LEDs in the next decade.

Another limitation factor in optical wireless transmitters based LED is the nonlinearity caused by thermal aspects. The LED has a threshold voltage, which is the minimum voltage to flow current across the LED and light emission. Below this voltage, the LED operate in cut-off region and above it, the current is increased exponentially as well as the light intensity toward saturation region. The LED current versus light power relation is nonlinear due to the thermal characteristic and the nonlinear transition into saturation region. This nonlinearity causes a drop in electrical to optical conversion and affects the modulated baseband signal represented by light intensity and hence, restricts the dynamic range and power transmission of optical transmitter. In conventional optical transmitter, a pre-distortion equalizer and post-equalization methods are used to decrease the signal distortion [3].

In RF communication system, a similar nonlinear effect was addressed. The power amplifier is a main source of nonlinearity when it operates near the saturation region causing a distortion in signal phase and amplitude [4]. Several linearization techniques are proposed to linearize the PA operation and increase the power efficiency such as, adaptive predistortion using LUT [5][6]. The LUT is an array of values, which are calculated based on linearization function needed to scale the amplitude and phase of the input signal and stored in memory. The creation of the LUT is done in a calibration mode. However, the updating could be done in real time to adjust to changing PA characteristics, such as a change in the temperature. For example, a cartesian LUT was proposed in [7] to eliminate the need for cartesian-to-polar conversion and modulator correction and reduces the power consumption of feedback path by allowing the use of low-speed low-SNR ADCs. In optical wireless systems, a look-up table coding method has been proposed to convert the information bits into the M-PPM codewords using a specially designed coding table. The utilization of M-PPM with forward correcting coding method increases system performance through constant power transmission. However, an exhaustive search using computer optimization method had to be done to find a subset of M-PPM codewords that satisfies the minimum hamming distance that defined according to system environment and the system purpose [8].

The OWC conventional transmitters employ DAC to transform the data bits into voltage and TCA to drive the optical source. The literature in [3] introduced a discrete power level stepping optical wireless OFDM transmitter, which consists of several LEDs groups that emit specific stepped optical intensities using switches driven by input data. This transmitter improves the system performance and reduces power consumption since DAC and TCA are no longer needs. This idea can be extended in our system to transmit an optical version of IR-UWB pulses.

In this paper, the employment of optical media to transmit a signal designed for IR-UWB radio system is investigated. To reach this goal, the electrical to optical conversion of pulse shapes using LUT is proposed. The proposed transmitter omits the DAC and quantization process needed for each pulse transmission as proposed in [1]. For a given modulation scheme, the signal pulse is stored in LUT and hence there is no need to repeat the same steps to convert the electrical Gaussian pulse to optical power. Also, the BER performance related to the size of LUT and quantization bit depth are presented. The IR-UWB structure of transmitter and receiver are discussed to elaborate system modification in seeks of optical link utilization. Moreover, the simulation of system is carried out to show the BER performance.

The reminder of the paper is organized as follows. In Section II, the system design describes the optical transmitter operation and quantization effects are presented. In Section III, the design of optical transmitter based LUT is introduced and in Section IV the system model including the optical channel impulse response regarding the environment and SNR are explained and analyzed. The system simulation is introduced and the results are discussed in Section V. Finally, Section VI concludes the paper.

II. SYSTEM DESIGN

Optical wireless systems consist of transmitter and receiver that employ optical parts mounted in front-ends as shown in Fig. 1. The transmitter modulate data information using one of single modulation schemes such as, (OOK, PAM, PPM, etc.) or multi modulation schemes such as, (OFDM, MPPM, M-PAM). These modulated symbols convert to analog signal that control the intensity of light emitted from an optical source such as LED or LD. The LD is preferred than LED, since it provides higher power, larger bandwidth, and linear electrical to optical characteristics at expense of eye safety limitation and higher cost. In the same manner, LEDs are low cost, higher lamination but limited bandwidth and suffer from nonlinearities of optical to electrical conversion characteristics. Table I summarizes the comparison of the two sources. Consequently, the receiver detects the optical light impinging on the surface and converts it to electrical current. Normally, the detector is p-intrinsic-n (PIN) photodiode or avalanche photodiode (APD). After the detector, low pass filter and amplifier are used to remove the higher frequency components and amplify the signal.

In the same manner, the IR-UWB transmitter sends the modulated symbol on a stream of short pulses shaped by pulse shape filter without carrier. One of modulation schemes (OOK, PPM, PAM, PSK, etc.) can be performed. After that, a Gaussian pulse or one of its derivatives is used to represent the modulated symbol. Also, multiple access methods such as, time hopping (TH) and direct sequence (DS) might be used along with modulation to increase the symbol power and range as well as enables multiple users. At the receiver, a correlation receiver or rake receiver employs to correlate signal shape with a local generated replica of pulse and hence obtain the detected bit using a decision rule.

To gain the benefits of these two systems, a modified IR-UWB over optical wireless links was proposed in [1]. This section illustrates the structure of system and introduces a solution for LEDs nonlinear effects.

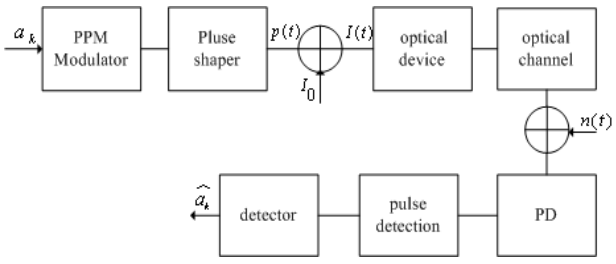

Figure 1. Optical IR-UWB system

TABLE I. COMPARISON OF LED AND LD

Characteristics	LED	LD
Output power	Low	High
Modulation bandwidth	10x-100x MHz	10x-100x GHz
Beam	Broad	Narrow
Coherence	Noncoherent	Coherent
Cost	Low	High
Harmonic distortion	High	Less

A. Transmitter Design

In a symbol time T_s, every data symbol is transmitted in form of N_f frames with frame duration T_f. In each frame, the information bits are modulated on short pulses $p(t)$ with pulse width T_p and $T_p \ll T_f$. The transmitter in Fig. 1 uses Pulse Position Modulation (PPM) with Gaussian shape pulse. The transmitted signal is represented as:

$$x(t) = p(t - kT_s - a_k\varepsilon) \quad (1)$$

In this modulation scheme, the transmitted pulse $p(t)$ is delayed for ε time shift, when the transmitted bit is one. In case of zero bits, the transmitter applies no delay to pulses. After signal modulation, the pulses enter pulse shaper that converts UWB pulses to be adequate for optical transmission. To transmit IR-UWB pulses over optical wireless link, the feed signal operates LED should be positive and above bias level. This means that any negative amplitude will bias light source reversely. Unfortunately, most of IR-UWB pulses are bipolar with negative and positive amplitudes. Nevertheless, the bipolar signal can be converted to unipolar by adding certain DC-bias that provides signal positivity as proposed in [1]. Although, large DC-bias increases signal power for a given BER while small DC-bias increases clipping noise causing signal distortion. Therefore, selection of DC-bias is tradeoff between signal power and clipping noise.

B. Optical pulse shaping

The signal pulse $p(t)$ is used to drive the LED by convert it to a set of quantized current levels as shown in Fig. 2. The pulse is quantized to L current level and every level is mapped to a defined brightness level. The current levels represent the intensity power should be non-negative to ensure that LED is not reversely biased.

$$I(t) = I_0 + p(t) \quad (2)$$

A dc-bias is chosen to boost the negative part of pulse in order to keep the LED in the 'ON' state and illuminance a 10% of full brightness. The constant forward current (I_0) will

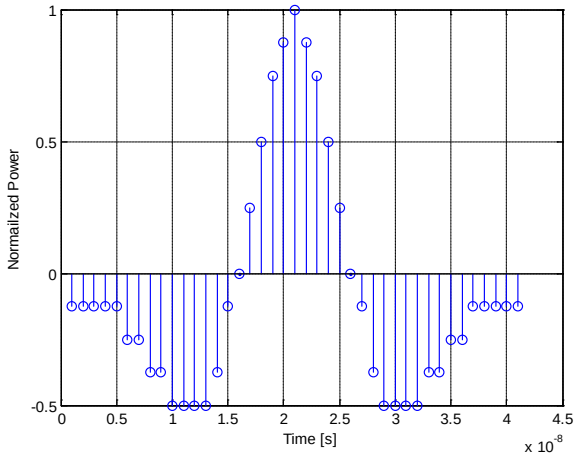

Figure 2. Quantization of the monocycle pulse.

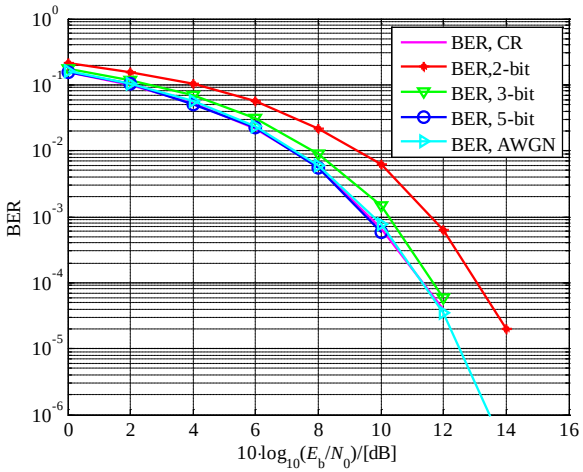

Figure 3. Efffects of quaintazition on BER performance.

keep LED operating even if the pulse time end and hence the LED remains working in the active region. Consequently, the modulation bandwidth should be increased since the LED switching times is minimized.

To create a different emission power according to current levels, we suggest the white-LED lnGaN/GaN to transmit the optical pulses. This white-LED as proposed in [9] shows that emission power in the blue spectrum portion is increased relative to the injected current. Nevertheless, a blue filter at the receiver front-end should be used to gain the blue spectrum power.

C. Quantization effects

The quantization of pulse plays important factor in system performance. The resolution of quantization defined by number of bits used to represent the quantization levels. Fig. 3 shows the BER performance of system employs a quantized pulse $p_o(t)$ at different bit resolution. The effect of channel is neglected to distingue the quantization effects and therefore, only optical noise is considered as additive

white Gaussian noise (AWGN). The simulation shows BER of Optical system at resolution of 2-bit, 3-bit, 5-bit, and analog signal (computer resolution). The result in Fig. 3 shows that every incremental bit reduces BER. After 5-bit, the error rate is close to that simulated with analog signal.

In the proposed transmitter in [1], the modulation is performed on bit level using PPM and IM is used to optically represent the signal shape in order to control the optical power derived by input current. However, this operation has to be carried out each time, which is power dissipative and time consume. Thus, we introduce a solution by storing the pulse samples values as binary codewords using LUT.

III. LOOK-UP TABLE TRANSMITTER

In this section, a look-up table is proposed to digitally store the quantized pulse in form of binary codewords that represents samples values. This design aims to increase the LED dynamic range and decrease the nonlinearities caused by transition to saturation region. Moreover, the transmitter complexity and electrical power consumption are expected to be minimized.

A. Transmitter structure

The proposed transmitter based LUT in Fig. 4 consists of PPM modulator, counter, and LUT connected to LED groups via resistors and switches. The LUT contains a number of codewords equal to pulse samples. The LUT input is connected to counter output, which address the LUT index. The counter is activated upon receiving modulated unit pulse from modulator. The modulator modulates zero bits as unit pulse with zero delay. Otherwise, the modulator shifts unit pulse by delay time ε. The counter feeds LUT with address of codeword that controls the total optical power of LEDs groups. The number of groups is defined by bit resolution specified in LUT design phase as will be discussed in the next subsection.

The output of LUT is digital binary vector that switch each group of LEDs (On/Off) based on the state of vector element (0/1). Also, each of these groups input current is scaled by a resistor R_N to emit different power levels P_N. Each group consists of number of LEDs N_{LED} to increase the optical power. The first group D_1 connected to most significant bit (MSB) and emits a maximum intensity power P_0 while D_1 emit half of P_0 and so on. The total emitted power is summation of power emitted by all active groups.

$$P_{total} = N_{LED} \sum_{n=1}^{N} P_n \quad (3)$$

$$P_n = \frac{P_{max}}{2^{n-1}} \quad (4)$$

For example, the codeword (10100) activates the first and third LED groups, while second; fourth and fifth remain in off state. The total optical power calculated using (3) and (4).

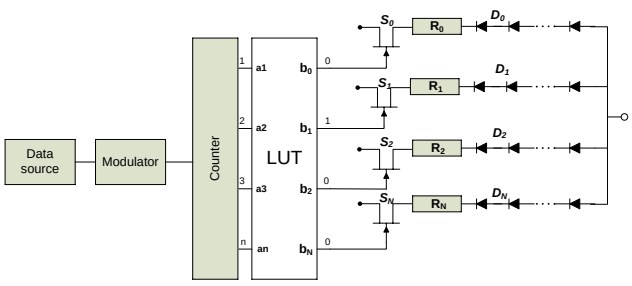

Figure 4. Optical IR-UWB transmitter based LUT.

B. Design of LUT

The LUT is used to store samples values as binary codewords. Fortunately, most of pulse shapes are symmetric, which minimize the LUT size to be adequate for only half of the pulse. This LUT design process is done in offline mode using computer simulations. However, a recalibration mechanism can be adopted to mitigate optical power nonlinearities and fluctuations as explained in next subsection. A digital representation of 5-bit quantized Gaussian pulse consists of 41 samples is sufficient to maintain a good performance as shown in Fig. 3. Table II illustrates a 5-bit binary codewords for half Gaussian pulse used in IR-UWB systems. The codeword length is optimized based on quantization bit depth that gives minimum SNR for a given BER. For example, a 5-bit codeword requires slightly less SNR compared to a 4-bit for BER of 10^{-4} at expense of large codeword length and hence LUT size that is determined by number of bits and number of samples. Although, the 4-bit codeword LUT transmitter needs four groups of LEDs and hence draws less power than 5-bit transmitter. The tradeoff between power consumption, size, and BER performance should be considered based on application. Also, several parameters should be taken in account in order to gain best performance such as, switching speed, resistors values, and maximum allowable LED input current, which are not discussed in this work.

C. LED Nonlinear effects

As mentioned in Section I, the LED suffers from limited dynamic range and nonlinear effects. For most of LEDs, the V-I curve has a limited linear range that can be used to modulate the signal power. This range can be extended further for a small range using predistortion techniques. However, the gain from this extension is not worthwhile, since only a small portion is achieved before the LED reaches the maximum allowable AC/pulsed current. In the proposed transmitter, the LED input current is fixed and scaled by resistors to keep LED operating in the linear region and controlling the total optical power by parallel switching of LEDs groups rather than direct current-power relation. However, the LED thermal behavior decreases the power conversion efficiency causing a drop in light intensity. To mitigate the thermal effects, the LUT should be recalibrated in the real-time to maintain constant optical power.

TABLE II. FIVE-BIT BINARY CODE REPRESENTATION OF GAUSSIAN PULSE.

Counter	Codeword
1	01111
2	01111
3	01111
4	01110
5	01110
6	01101
7	01100
8	01011
9	01010
10	01001
11	01000
12	01001
13	01001
14	01011
15	01110
16	10001
17	10101
18	11001
19	11101
20	11111

The emitted optical power is generated according to digital codewords, and hence can be digitally adjusted or corrected to emit more or less power. This can be done by adding one more bin to the output of LUT connected to an extra LED group for intensity correction. This additive group compensates the optical power in case of power fluctuations using real-time measurements for the emitted power via optical sensor. The data is sent back through feedback as a digital codeword to compare it with the current values. Moreover, the LUT values can be also updated based on the measurements to obtain more power efficiency. As a result, the nonlinear effect from LED whether thermal or electrical can be mitigated and constant optical power will be achieved.

IV. SYSTEM MODEL

For any wireless communication system, the multipath channel differentiates the transmitted and received signal. The path loss and dispersion determines the system design parameters. This section describes the modeling of optical wireless system in indoor environment. A simulation of channel impulse response and SNR in an office room will be discussed. Also, the receiver design for the proposed system including the optical front-end will be presented.

A. Optical Multipath Channel

The optical multipath channel is characterized by an impulse response $h(t)$, which describes the propagation of optical signal between the transmitter and receiver. The propagation pattern is approximated by lambertian radiation pattern, which state that the light intensity emitted from a source has a cosine dependence on the angle of emission with respect to the surface normal [10][11]. The luminous intensity in angle ϕ is given by

$$I(\phi) = I(0)cos^m(\phi) \tag{5}$$

where $I(0)$ is the center luminous intensity of the LED and ϕ is the angle of irradiance, m is the order of lambertian emission and is given by the semi angle at half illuminance of the LED $\phi_{1/2}$ as

$$m = \frac{-\ln(2)}{\ln(\cos\phi_{1/2})} \tag{6}$$

and the horizontal illuminance I_{hor} at a point (x, y, z) on the working plane is defined as

$$I_{hor}(x, y, z) = \frac{I(0)cos^m(\phi)}{d^2\cos(\psi)} \tag{7}$$

where d is the distance between the transmitter and receiver and ψ is the angle of incidence.

In an office room environment, the light arrive receiver directly (LOS link) or after number of reflections (diffuse link). The impulse response at zero reflection is given as:

$$h_{los} = \frac{A_r(m+1)}{2\pi d^2}cos^m(\phi)T_s(\psi)g(\psi) \cdot \cos(\psi)\delta\left(t - \frac{d}{c}\right). 0 \le \psi \le \psi_{con} \tag{8}$$

where $T_s(\psi)$ is the filter transmission, $g(\psi)$and $\psi_{con}$are the concentrator gain and field of view (FOV), respectively. The gain of the optical concentrator at the receiver is defined by:

$$g(\psi) = \begin{cases} \frac{n^2}{\sin^2\psi_{con}}, & 0 \le \psi \le \psi_{con} \\ 0, & 0 \ge \psi_{con} \end{cases} \tag{9}$$

where n is the refractive index. To model the reflections, every wall is partitioned to a number of small areas. Each one acts as new lambertian source when light incident on it. The impulse for the first reflection is given by:

$$h_{ref}(t) = \begin{cases} \dfrac{A_r(m+1)}{2(\pi d_1 d_2)^2}\ \rho\ A_{wall}\ cos^m(\phi_r)\ \cos(\psi_r) \\ \cos(\alpha_{ir})\cos(\beta_{ir})\ T_s(\psi)\ g(\psi_r) \\ \delta\left(t - \dfrac{d_1 + d_2}{c}\right), \qquad 0 \le \psi_r \le \psi_{con} \\ 0, \qquad\qquad\qquad \psi_r \ge \psi_{con} \end{cases} \tag{10}$$

where d_1 and d_2 are the distances between the LED and a reflective point, and between a reflective point and a receiver surface, ρ is the reflectance factor, A_{wall} is a reflective area. The angles α_{ir} and β_{ir} represent angle of incidence to a reflective point and angle of irradiance to a receiver, respectively, ϕ_r and ψ_r are the angle of irradiance from LED to a reflective point and angle of incidence from reflective point to a receiver.

The optical channel is characterized by the room dimensions, reflectance indices of walls, and transmitter and receiver orientation. Table III describes the parameters used to simulate the channel impulse response. The optical impulse response is used to calculate the channel gain, which is important to estimate the influence of channel on the received power. The power contained in a LOS component h_{los} is larger than the power contained in first reflection components h_{ref} as shown in Fig. 5. The long distance and reflection from the surfaces introduce power loss and longer delay. The received power in NLOS case can be calculated as sum of LOS and NLOS pathlosses multiplied by transmission power. The received power can be expressed as

$$p_r = \left(p_t H_{los}(0) + \int p_t H_{ref}(0)\right) \tag{11}$$

where p_t represents transmitted power, and $H_{los}(0)$, $H_{ref}(0)$ represent power in direct and reflected paths, respectively.

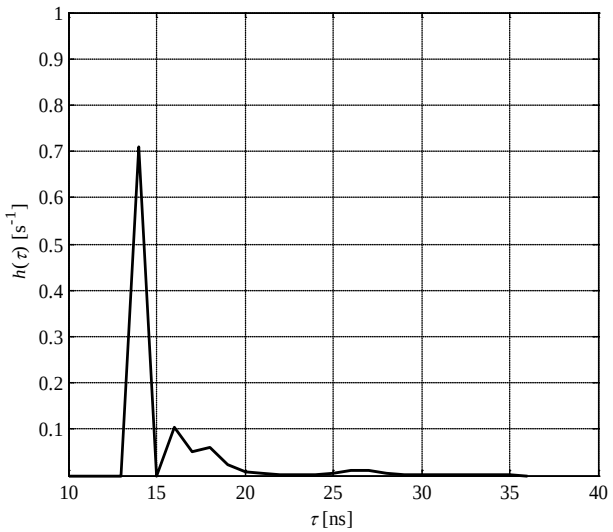

Figure 5. Optical channel impulse response.

Another important future is the root mean squared (RMS) delay, which describes how much delay added by the channel. A large delay led to ISI, which make the detection of transmitted signal complicated. The RMS delay calculated from the channel impulse response as

$$\tau_{rms} = \sqrt{\frac{(t-\tau_0)^2 h^2(t) dt}{\int h^2(t) dt}} \tag{12}$$

where τ_0 is mean delay time defined by:

$$\tau_0 = \frac{\int t\ h^2(t) dt}{\int\ h^2(t) dt} \tag{13}$$

Using equations (12), (13) and parameters in Table III, RMS delay time can be calculated in case of LOS and NLOS channel as shown in Fig. 6 and Fig. 7. This parameter determines the upper bound of transmission rate. For the proposed system, the symbol time is more than the simulated RMS delay time in case of LOS scenario. Hence, equalization stage is not necessary.

TABLE III. THE CHANNEL PARAMETERS.

	Parameter	Value
Room	Room size	5×5×3 m^3
	ρ_{wall}	0.8
Transmitter	Location	(2.5, 2.5, 3)
	M	1
	Elevation	-90°
	Azimuth	0°
	Power	1
Receiver	Location	(0.5,1,0)
	A_r	1 cm^2
	FOV	60°
	Elevation	90°
	Azimuth	0°

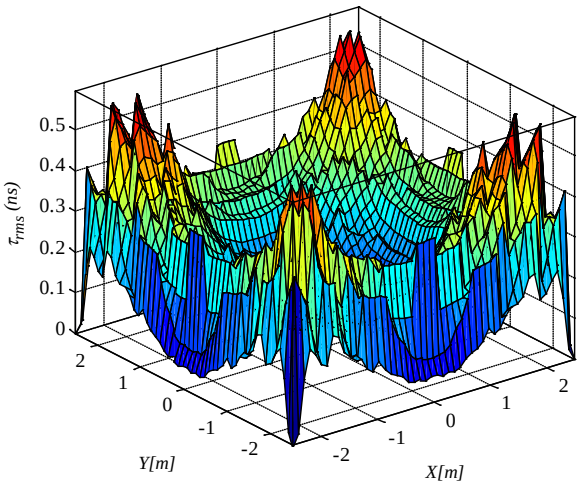

Figure 6. RMS delay for LOS configuration.

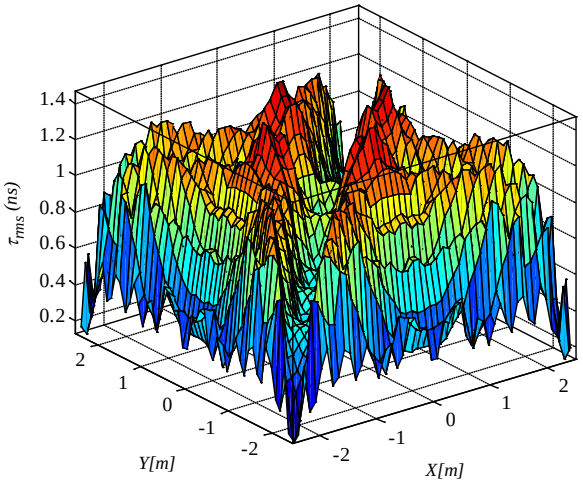

Figure 7. RMS delay for NLOS configuration

B. SNR

In optical systems, SNR is defined by received power p_r, photodiode responsivity [A/W], and noise variances of the shot noise σ_{sh}^2 and thermal noise σ_{th}^2 as [12]

$$SNR = \frac{(Rp_r)^2}{(\sigma_{sh}^2 + \sigma_{th}^2)} \quad (14)$$

The noise sources are classified into two types namely shot noise and thermal noise. The shot noise is a time-varying process generated by external light sources like background noise and quantum noise or internal source as intensity radiation, dark noise and excess noise. These sources are independent Poisson random variables and their photoelectron emission follows the distribution of Poisson distribution with mean equal to the sum of the individual processes. The variance of any shot noise process associated with photodetection is represented as [12]:

$$\sigma_{sh}^2 = 2qB\langle i \rangle \quad (15)$$

where q is the electronic charge, and B is the equivalent bandwidth, and $\langle i \rangle$ is the mean current generated by $\langle n \rangle$ electron. However, if the photoelectron count is large, the generated signal current probability distribution can be approximated as Gaussian process [12].

$$p(i) = \frac{1}{\sqrt{2\pi\sigma_{sh}^2}} exp\left(\frac{[i - \langle i \rangle]^2}{2\sigma_{sh}^2}\right) \quad (16)$$

In addition to the shot noise, the thermal noise caused by thermal fluctuation of electrons in receiver circuit generates a random current, which is modeled as Gaussian process has a zero mean and its variance described as

$$\sigma_{th}^2 = \frac{4\kappa T_k B}{R_L} \quad (17)$$

where κ is Boltzmann's constant, T_k is absolute temperature, and R_L is the equivalent resistance. The total generated current probability distribution of thermal noise and shot noise can be represented as in [12]

$$p(i) = \frac{1}{\sqrt{2\pi[\sigma_{sh}^2 + \sigma_{th}^2]}} exp\left(\frac{[i - \langle i \rangle]^2}{2[\sigma_{sh}^2 + \sigma_{th}^2]}\right) \quad (18)$$

To evaluate channel variations, the room is partitioned to small areas equal to 225. The channel power is simulated using parameters in Table III. The received power in any place in room of size (5m×5m×3m) is estimated as shown in Fig. 8. The minimum received power is -2.3dBm at corners while maximum received power reaches 2.6dBm in room center. The utilization of large number of LEDs provides high received power that is required for good quality communications. However, multiple sources results in path difference that leads to ISI at the receiver and degrade the performance [13].

The received power needed to achieve a BER of 10^{-6} in PPM modulation is to be calculated as [13]:

$$BER = Q\left(\sqrt{SNR}\right) \quad (19)$$

As shown in Fig. 9, the range of SNR is between 11dB and 40dB for a total power summation of LOS path and NLOS paths. The noise parameters required to calculate shot noise and thermal noise are illustrated in [13]. The SNR is obtained using received power shown in Fig. 8 and calculated noise power. The proposed system can achieved the required low data rate at minimum data errors. In absence of LOS power, the received power is reduced dramatically.

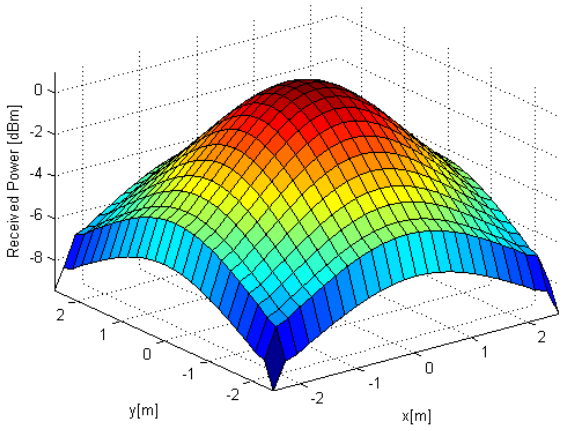

Figure 8. Received optical power.

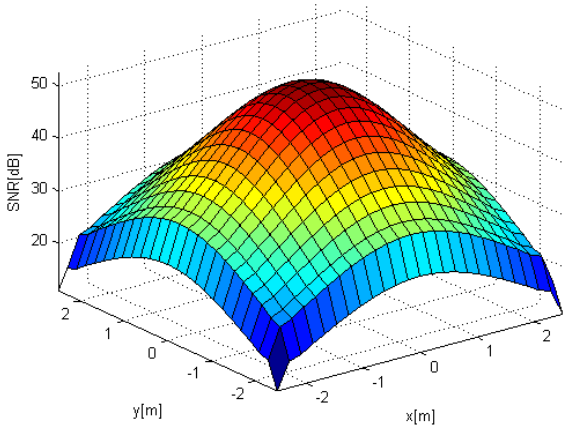

Figure 9. Simulation of SNR.

C. Receiver Design

The receiver of optical wireless system shown in Fig. 10 is based mainly on photodiode (PD) employing the direct detection. The detector area and the orientation play important role in the receiver design and performance. The PD generates an output photocurrent relative to the incident light power pinging on the surface, i.e., the changes produced in intensity modulation at the transmitter are detected by direct detection at the receiver. The photocurrents induced by PD form a replica of the transmitted pulse. At the receiver front-end, the received signal is defined as

$$y(t) = R\, I(t) * h(t) + n(t) \tag{20}$$

The transmitted current signal $I(t)$ is convoluted with optical multipath channel $h(t)$, and added to AWGN $n(t)$. After conversion of optical signal to electrical signal in receiver, the correlation between the mask of transmitted pulse and the

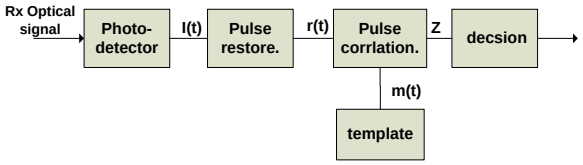

Figure 10. Optical IR-UWB Receiver

received signal is performed as:

$$m(t) = I(t - \tau - kT_s) - I(t - \tau - kT_s - \varepsilon)$$
$$Z = \int_{\tau}^{T_s+\tau} y(t)m(t)dt \tag{21}$$

The detector compares the power of correlation to a threshold and decides whether the received bit is '0' or '1' [14].

$$\hat{a} = \begin{cases} Z > 0, & \hat{a} = 0 \\ Z < 0, & \hat{a} = 1 \end{cases} \tag{22}$$

V. Simulation and Results

In this section, we simulate system design presented in [1] and the proposed system using transmitter based LUT. Both systems are simulated using Monte Carlo simulation in Matlab program.

The system design represented in Fig. 1 is simulated using MATLAB program. In this design, the transmitter based LUT method substitutes the former one presented in [1]. The Monte Carlo simulations were carried out to generate the bit-error-ratio (BER) versus E_b/N_0 results. The information bits are modulated by 2-PPM modulator with symbol time $T_s = 240ns$. The sampling frequency $f_c = 1GHz$ and shift time $\varepsilon = 120ns$, $N_f = 1$. The monocycle Gaussian pulse is used with width $T_p = 41ns$. The pulse samples are quantized to $L = 32$ current levels and stored in LUT as binary codeword. These code words drive five LED groups each consists of eight LEDs. Each of these groups emits a different power level that contributes in evaluation of the intended pulse sample value as explained earlier. The optical channel impulse response in Fig. 5 is simulated in a room with dimensions of (5m×5m×3m) and a fixed transmitter and receiver are assumed. The optical pulse is convolved with the channel and added to the noise.

On the receiver side, the photodiode is percepts the incident light and converts it into current. We assume that the detector responsivity R equal to one. The received pulse constructed from current levels is correlated with the mask of transmitted pulse and the peak power is compared to the threshold in time window. This system is assumed to be synchronized and no equalization stage is performed.

In OWC systems, a unit rectangular pulse is used to transmit the power of modulated binary bits with duration

T_s as proposed in [15][16]. In Fig. 11, the same system design was simulated using rectangular pulse and monocycle pulse to compare the BER performances of using the shaped pulse used for wireless system and rectangular pulse used in OWC systems. Fig. 11 shows that the BER for both signals are equal because of power direct detection, which is evident that other pulses shape could be used without loss of performances. Although rectangular pulse evaluation is simpler than Gaussian pulse, the later introduces capability for utilizing advantages of a designed UWB radio wireless system communicating on optical link in sensitive environments. Nevertheless, effects of LEDs nonlinearities and shot noise are expect to disfigurement the transmitted Gaussian pulse at transmitter and receiver front-ends. These effects will be studied experimentally in the future work to find the performance degradation for the proposed design. Fig. 12 compares the BER performance of the proposed systems operate on LOS optical wireless channel with that on diffuse channel in the absence of LOS link. The direct path between transmitter and receiver delivers higher power than paths reach the PD after reflections. This explains why the BER in the presence of LOS channel is lower than that in diffuse channel by ~2dB. Also, the influences of optical wireless channel gain and delay on the proposed system increase the BER by ~4dB compared to the AWGN bound.

The second simulation determines BER performances for the proposed design in case of channel variation during data transmission. In this case, the mobile user changes her/her location inside office environment with dimensions listed in Table III. Therefore, we simulate channel impulse responses for 2500 points that represent possible receiver's location in X-Y plane. The channel is simulated between fixed transmitter and receiver locations.

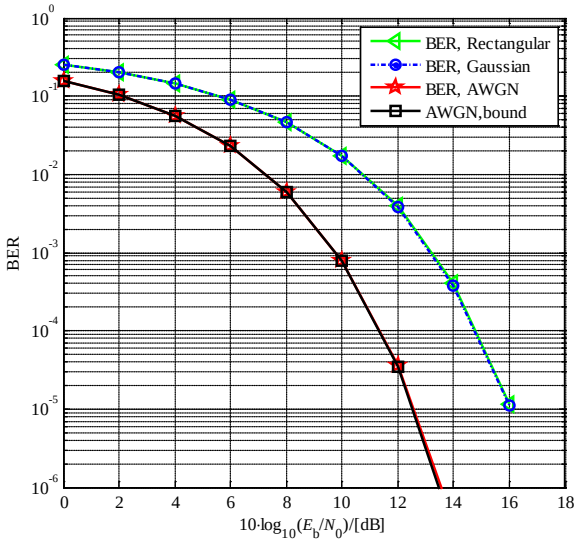

Figure 11. BER of the system with rectangular and Gaussian Pulses.

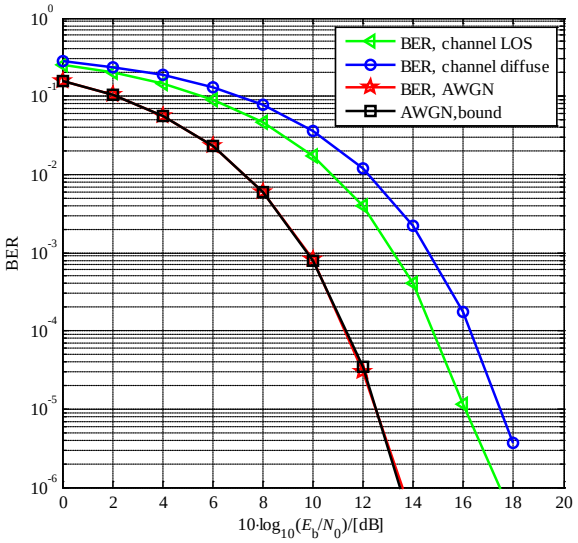

Figure 12. BER of the system with LOS and diffuse link configurations

Moreover, we have distinguished two scenarios for each observation. First, the LOS link is not blocked by obstacles and both of direct radiation and reflected radiations are present. In the second scenario, NLOS link was established and only reflected radiation is received regardless receiver's position. In Fig. 13 and Fig. 14, the channel impulse responses are depicted. As seen from figures, the channels in second scenario experiences a larger pathloss than in first scenario due to diffusion phenomena in NLOS case and absence of LOS power contribution, which contain largest portion of received signal. Nevertheless, the system simulation for first scenario is done over 2500 channels. We assume that a channel response changes once within frame time duration $T_s = 240ns$. The user's location number is determined as uniform random variable.

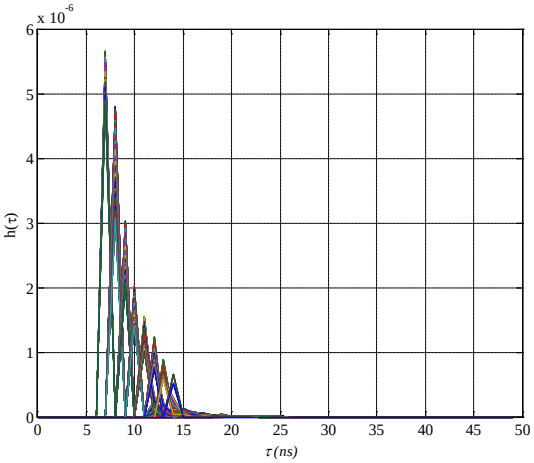

Figure 13. Channel impulse responses for LOS and NLOS links.

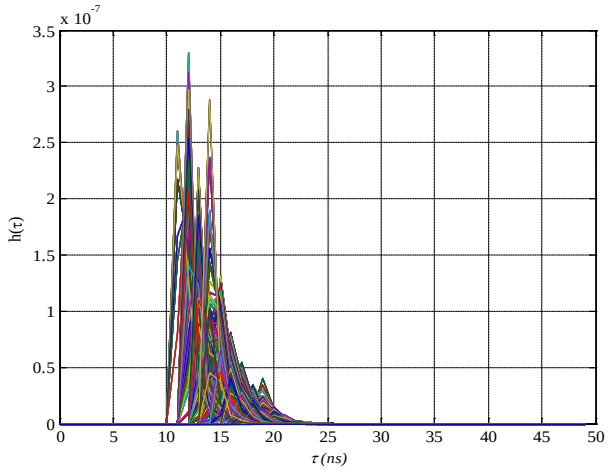

Figure 14. Channel impulse responses for NLOS links

.

Fig. 15 shows system's BER under channel response composed of LOS and NLOS radiations. Likewise, the system is simulated for second scenario where LOS link is shadowed over transmission time. Fig. 15 shows larger BER than presented by first scenario due to larger channel pathloss and delay. A third case is simulated, when channel changes over 5000 channel observations simulated in first and second scenarios. The channel configuration and user's location is determined as uniformly-distributed random variable. This case is more realistic where channel response varieties between two scenarios presented above. During user mobility, the user moves in an office where some positions are shadowed by obstacles or sudden obstacle is taken place. The system BER is closely better to that presented in second scenario as shown Fig. 15. These scenarios summarized system's BER performance for mobile user situation. It worthwhile to recall that, the user's location is randomized as uniform-distributed random variable.

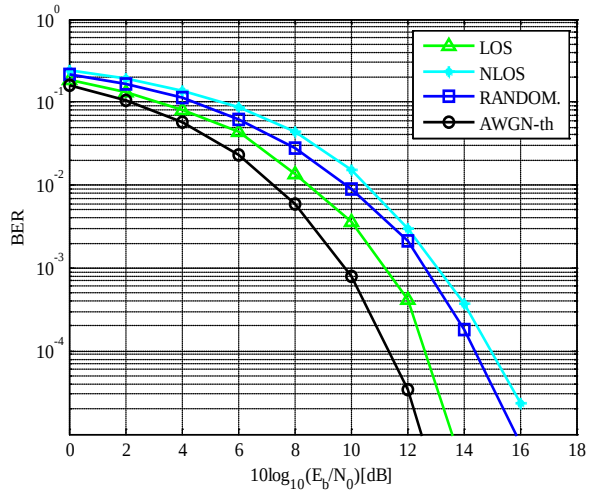

Figure 15. BER of proposed system in mobility scinarios

VI. CONCLUSIONS AND FUTURE WORKS

In this paper, an optical wireless transmitter based LUT was introduced. The radio system pulse was translated to binary codewords stored in LUT. The needs for ADC and TCA were excluded as well as pulse reformation for each symbol time. The utilization of LUT enables more linear characteristics of LEDs. The transmitter complexity and power consumption were reduced as compared with transmitter employing DC-bias and direct quantization. The optical multipath channel was investigated and the system performances using Monte-Carlo simulations have been obtained and analyzed. Also, the BER performances for fixed and mobile user in office environment were simulated and analyzed. This design will be suitable for non-radio environment like hospitals or for systems that operate in both optical/radio configurations. This work will be continued to evaluate better performance using predistortion techniques to adapt the LUT and hence more linearity for LEDs power.

REFERENCES

[1] M. Al-Olofi, A. Waadt, G. H. Bruck, and P. Jung, "Design of optical wireless IR-UWB wystems for Low Data Rate applications," Proc. of the Ninth Advanced International Conference on Telecommunications AICT 2013, pp. 7-12, Rome 2013, ISBN: 978-1-61208-279-0

[2] C. L. Liao, Y. F. Chang, C. L. Ho, and M. C. Wu, "High-Speed GaN-Based Blue Light-Emitting Diodes with Gallium-Doped ZnO current spreading layer," Electron Device Letters, IEEE , vol. 34, no. 5, pp. 611-613, May 2013 doi: 10.1109/LED.2013.2252457.

[3] T. Fath, C. Heller, and H. Haas, "Optical wireless transmitter employing discrete power level stepping," Journal of Lightwave Technology, vol. 31, no. 11, pp. 1734,1743, June, 2013 doi: 10.1109/JLT.2013.2257984

[4] Z. Zhu and X. Huang, "Design of an LUT-Based predistorter for power amplifier linearization," Advances in Satellite and Space Communications, 2009, pp. 113-116, July 2009, doi: 10.1109/SPACOMM.2009.13

[5] J. K. Cavers, "Amplifier linearization using a digital predistorter with fast adaptation and low memory requirements," IEEE Trans. Veh. Technol., vol. 39, no. 4, pp. 374-382, Nov. 1990.

[6] K. J. Muhonen, M. Kavehrad, and R. Krishnamoorthy, "Look-up table techniques for adaptive digital predistortion: A development and comparison," IEEE Trans. Veh. Technol., vol. 49, no. 9, pp. 1995-2002, Sep. 2000.

[7] S. W. Chung, J. W. Holloway, and J. L. Dawson, "Energy-Efficient Digital Predistortion With Lookup Table Training Using Analog Cartesian Feedback," IEEE Transactions on Microwave Theory and Techniques, vol. 56, no. 10, pp. 2248-2258, Oct. 2008, doi: 10.1109/TMTT.2008.2003139

[8] H. F. Rashvand, Y. Zeng, R. J. Green, and M. S. Leeson, "Look-up table error correcting multiple pulse PPM codes for wireless optical communication channels," IET , vol. 2, no. 1, January 2008, pp. 27-34, doi: 10.1049/iet-com:20060386

[9] J. Grubor, S. C. J. Lee, K. D. Langer, T. Koonen, and J. W. Walewski, "Wireless high-speed data transmission with phosphorescent white-light LEDs," in Proc. Eur. Conf. Optical Communications (ECOC 2007), Berlin, Germany, Sept. 2007, pp. 1-2.

[10] J. R. Barry, J. M. Kahn, W. J. Krause, E. A. Lee, and D. G. Messerschmitt, "Simulation of multipath impulse response for

wireless optical channels," IEEE J. Select. Areas in Communications, vol. 11, no. 3, Apr. 1993, pp. 367–379, doi: 10.1109/49.219552.

[11] H.Q. Nguyen, J. Choi, M. Kang, Z. Ghassemlooy, D. H. Kim, S. Lim, T. Kang, and C. G. Lee, "A MATLAB-based simulation program for indoor visible light communication system," CSNDSP 2010 Proceedings, July 2010, pp. 537-541.

[12] Z. Ghassemlooy, W. Popoola, and S. Rajbhandari, Optical wireless communications: system and channel modelling, CRC Press, 2012, pp. 66-74.

[13] T. Komine and M. Nakagawa, "Fundamental analysis for Visible-Light Communication system using LED light," IEEE Transaction on Consumer Electronics, Vol. 50, No. 1, February 2004, pp. 100-107, doi: 10.1109/TCE.2004.1277847.

[14] M. G. Di Benedetto, Understanding Ultra Wide Band radio fundamentals, Pearson Education, 2008, pp. 241-252.

[15] M.D Audeh, J.M Kahn, and J.R. Barry, "Performance of pulse-position modulation on measured non-directed indoor infrared channels," IEEE Transactions on Communications, vol. 44, no. 6, Jun. 1996, pp. 654-659, doi: 10.1109/26.506380.

[16] J. Zhang, "Modulation analysis for outdoors applications of optical wireless communications," International Conference on Communication Technology Proceedings, 2000. WCC - ICCT 2000, vol. 2, no. 2000, pp. 1483-1487, doi: 10.1109/ICCT.2000.890940.